

Inverse analysis of the heat conduction process induced by impinging jet

M. WOELKE ⁽¹⁾, L. BOGUSŁAWSKI

*Poznań University of Technology, Chair of Thermal Engineering,
ul. Piotrowo 3, 60 -965 Poznań,
e-mail: woelkem@sol.put.poznan.pl*

THIS PAPER PRESENTS an analysis of the cooling process of a solid, induced by the impingement of an air jet. Solutions of the inverse heat conduction problem were obtained by applying the heat functions to formulate the base functions of the Finite Element Method. The applied heat functions identically satisfy the heat conduction equation in dimensionless co-ordinates. The minimisation of the functional, presented in this paper, leads to the solutions of the analysed problem. The temperature distribution of the analysed solid was determined by solving the inverse heat conduction problem by means of the temperature measurements taken inside the solid. Properties of the heat function were applied to reconstruct the distribution of the Bi number on the heat exchange surface; this in turn enables to determine the heat transfer coefficient on the analysed surface. The results of the analysis were compared with the data found in the literature.

Notations

a	temperature compensatory coefficient,
$Bi = \frac{hZ}{k}$	Biot's number,
c	velocity,
g	temperature gradient,
h	heat transfer coefficient,
i	number of the nodes,
I	direct functional,
J	inverse functional,
j	number of measurement points,
k	heat conduction coefficient,
K	number of finite elements,
l	number of the heat functions,
L	final number of finite elements,,
m	final number of measurement points,
n	time step,
N	final number of the nodes in each finite element,

¹⁾Graduate from study for doctor degree at PUT

p	parameter,
q	density of the heat flux,
t	time,
T	temperature surplus,
w	generating function,
z	characteristic dimension for the heat conduction,
Z	length of the analysed solid in the heat conduction direction,
<i>Greek letters</i>	
δ	standard deviation,
θ	approximate value of the temperature surplus,
θ^n	approximate value of the temperature surplus from n time step,
$\xi = \frac{z}{Z}$	dimensionless co-ordinates,
$Fo = \tau = \frac{a}{Z^2}t$	Fourier's number,
v	heat function,
$\varphi_i(\xi, \tau)$	base function of FEM,
Ω	surface of the finite element.

1. Introduction

THE CONCEPT OF SOLUTION of the inverse heat conduction problem implies the determination of the unknown boundary condition on the basis of the temperature measurements taken inside the solid. The inverse heat conduction problems are ill-posed; it means that small changes of the temperature inside the solid could correspond to larger changes of the temperature on the heat exchange surface. As a consequence, small uncertainty in temperature measurements taken inside the solid causes significant errors in temperature on the heat exchange surface determined by the solution of the inverse problem. The inverse heat conduction problems are analysed in the papers [2, 3, 4, 5, 8, 9, 10, 12, 13, 14].

The determination of the heat exchange boundary conditions, on the surface cooled by impinging air jet, is based on solving the inverse heat conduction problem.

The temperature field satisfies the equation

$$(1.1) \quad \frac{\partial^2 T(\xi, \tau)}{\partial \xi^2} = \frac{\partial T(\xi, \tau)}{\partial \tau}, \quad \tau > 0, \quad \xi \in (0, 1)$$

and is subjected to the initial condition

$$(1.2) \quad T(\xi, 0) = T_p(\xi, 0), \quad \xi \in \langle 0, 1 \rangle$$

and to the boundary condition

$$(1.3) \quad \frac{\partial T(0, \tau)}{\partial \xi} = 0 \quad \text{for } \xi = 0, \tau > 0,$$

$$(1.4) \quad T(1, \tau) = T_B(1, \tau) \quad \text{for } \xi = 1, \tau > 0.$$

The boundary condition (1.4), in the inverse problem, was investigated by experimental studies.

The problem was analysed in dimensionless co-ordinates $Bi = \frac{hZ}{k}$ (Biot's number), $\xi = \frac{z}{Z}$ and $Fo = \tau = \frac{a}{Z^2}t$ (Fourier's number).

The determination of the boundary condition for $\xi=1$ leads, by means of the heat functions properties, to the determination of the heat transfer coefficient h on the heat exchange surface.

Due to complexity of the geometry conditions of the heat machines, the determination of the heat transfer coefficient h is complicated, because the mounting of the measurement sensor might be very difficult.

2. Numerical analysis of the heat transfer

The solution of the inverse heat conduction problem consists in the solution of the direct problem with the unknown boundary conditions as a parameter.

The unknown boundary condition is determined by minimisation of the difference between the temperature calculated and the experimental temperature measurements [5].

2.1. Determination of the direct problem

The temperature field in a flat layer is analysed in order to solve the direct heat conduction problem. The temperature field satisfies the heat Eq.(1.1) with boundary conditions (1.3), (1.4) and initial condition (1.2). The area of the solution of the analysed problem is shown in Fig. 1.

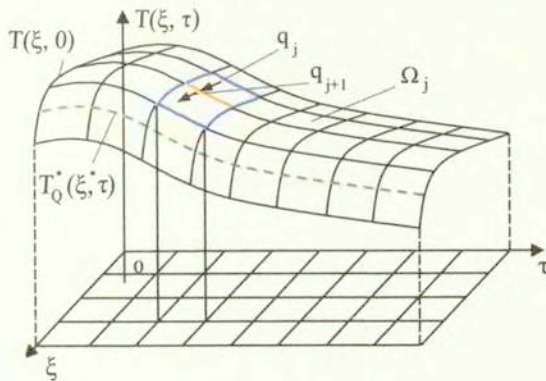


FIG. 1. The discreet area of the solution of the analysed problem.

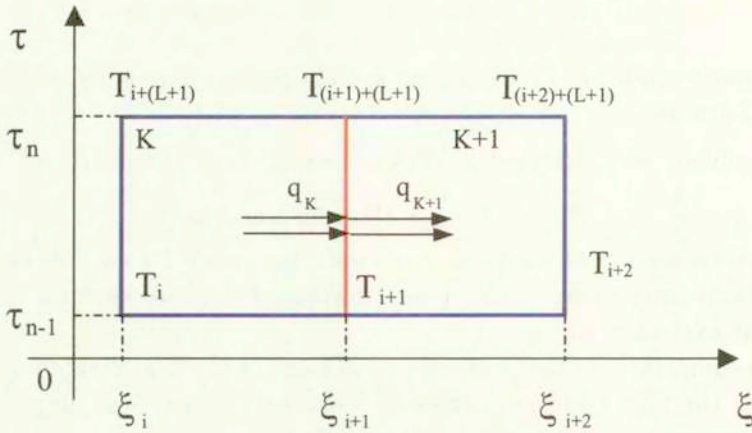


FIG. 2. Two finite elements of the discretized area of the solution of the analysed problem.

In this paper, the results of the analyses are presented for the finite element consisted of four nodes, but the number of nodes in each finite element could be $N=4, 6, 8$.

Approximation of the temperature in the element K of the analysed area may be presented in the form

$$(2.1) \quad \theta_K(\xi, \tau) = \sum_{i=1}^N \varphi_i^K(\xi, \tau) T_i \quad \text{for } K = 1, \dots, L.$$

The heat functions were used to determine the base function $\varphi_i(\xi, \tau)$ of Finite Element Method. The heat functions are obtained by expansion in series of generating function $\exp(p\xi + p^2\tau)$ [4]

$$(2.2) \quad w(\xi, \tau, p) = e^{p\xi + p^2\tau} = \sum_{l=1}^{\infty} v_l(\xi, \tau) \cdot \frac{p^l}{l!} \quad \tau \geq 0, \quad \xi \in (0, 1)$$

where coefficients of the series (2.2) are found from the formulae [4]

$$(2.3) \quad v_{l+1}(\xi, \tau) = \frac{\xi}{l} \cdot v_l(\xi, \tau) + \frac{2\tau}{l} \cdot v_{l-1}(\xi, \tau), \quad l \geq 2,$$

$$v_0 = 0, \quad v_1(\xi, \tau) = 1, \quad v_2(\xi, \tau) = \xi,$$

$$\frac{\partial v_l(\xi, \tau)}{\partial \xi} = v_{l-1}(\xi, \tau), \quad \frac{\partial v_l(\xi, \tau)}{\partial \tau} = v_{l-2}(\xi, \tau), \quad l = 1, 2, 3, \dots$$

The heat functions determined above, identically satisfy Eq. (1.1). The base functions of the Finite Element Method are formed as linear combinations of the heat functions. Therefore the basic functions automatically satisfy the heat conduction equation (1.1)[4].

For the purpose of determination of unknown temperatures at the nodes of finite elements mesh, the following functional was minimised:

$$\begin{aligned}
 (2.4) \quad I = & \int_{\tau}^{\tau+\Delta\tau} \left(\frac{\partial \theta_1(0, t)}{\partial \xi} - 0 \right)^2 dt \\
 & + \int_{\tau}^{\tau+\Delta\tau} (\theta_{K=L}(1, t) - T_B(1, t))^2 dt + \sum_{K=1}^L \int_{\xi_K}^{\xi_{K+1}} (\theta_K(\xi, 0) - T_p(\xi, 0))^2 d\xi \\
 & + \sum_{K=1}^L \int_{\tau}^{\tau+\Delta\tau} \left[-\frac{\partial \theta_K(\xi_g, t)}{\partial \xi} + \frac{\partial \theta_{K+1}(\xi_g, t)}{\partial \xi} \right]^2 dt,
 \end{aligned}$$

Minimisation of the functional (2.4) with respect to unknown temperatures at the nodes of finite elements mesh leads to solutions of the direct heat conduction problem. The solution of the direct problem demonstrates the relation between the temperature of the previous time step and the boundary condition

$$(2.5) \quad \{\theta^n\} = [DD] \{\theta^{n-1}\} + [GB] T_B^n + [GA] T_B^{n-1}.$$

Most significant is the relation between the solution of the direct heat conduction problem (2.5) and the boundary condition (1.4) for $\xi=1$.

2.2. Determination of the inverse problem

The temperature $T_B^n(\tau_n)$ is sought by solving the inverse heat conduction problem. The temperature inside the solid should be measured for the purpose of solving the inverse heat conduction problem. The measurements of the $T_Q^*(\tau_n)$ temperature were performed to build the functional, the minimisation of which leads to the determination of the temperature distribution of the solid

$$(2.6) \quad J = \|\theta_K(\xi^*, \tau_n) - T_Q^*(\tau_n)\|^2 = \sum_{j=1}^m (\theta_K(\xi^*, \tau_n) - T_Q^*(\tau_n))_j^2.$$

Here j – the number of measurement points (ξ^*, τ_n) of the $T_Q^*(\tau_n)$ temperature (here the analysis was accomplished for $m=1$).

Minimisation of the functional (2.6) with respect to the unknown temperature $T_B^n(\tau_n)$ leads to the solution of the inverse heat conduction problem

$$(2.7) \quad \{\theta^n\} = [GDD] \{\theta^{n-1}\} + \sum_{j=1}^m [GNN]_j \cdot T_{Q,j}^* + [GT] \cdot T_B^{n-1}.$$

In the paper [14] were published the results of the solution of the inverse problem, calculated by means of the numerically generated temperature measurements. The size of this stability area of solution of the inverse problem was determined as a function of localisation of the temperature measurement sensor. The obtained results confirm the applicability of the heat functions to analyse the heat conduction equation.

3. Experimental analysis

The heat transfer process analysed in this paper consists in conducting heat by the solid through the heat exchange surface and taking over the heat by the impinging cooling air jet. The experimental research was aimed at validation of the applicability of the inverse analyses solved by means of the heat function to examine the heat exchange intensification on the analysed surface.

For the purpose of ensuring one-dimensional heat conduction, heat transfer through the thickness of the flat plate was replaced by the heat transfer along the length of the cylinder.

The change of the shape of the analysed solid is negligible for the solution validity. It simplifies the fulfilment of the assumed heat transfer boundary conditions. Due to this change, the shape of the analysed solid was adjusted to the shape of the impinging air jet.

In the experimental research, the temperature was measured along the symmetry axis of the cylinder in five measurement points. The temperature measurements were taken for solving the inverse heat conduction problem and for the assessment of validity of the obtained solution. The locations of the measurement points are shown in Table 1 and Fig. 3.

Table 1. The locations of temperature measurement points

Location of temperature measurements	z=1mm	z=2mm	z=3mm	z=20mm	z=40mm
	$\xi = 0.983$	$\xi = 0.978$	$\xi = 0.950$	$\xi = 0.667$	$\xi = 0.334$

The analysed solid was made of 0H18N9 steel ($\lambda = 14,65 \text{ W/mK}$), with length $Z=0,6\text{m}$ chosen as a characteristic dimension.

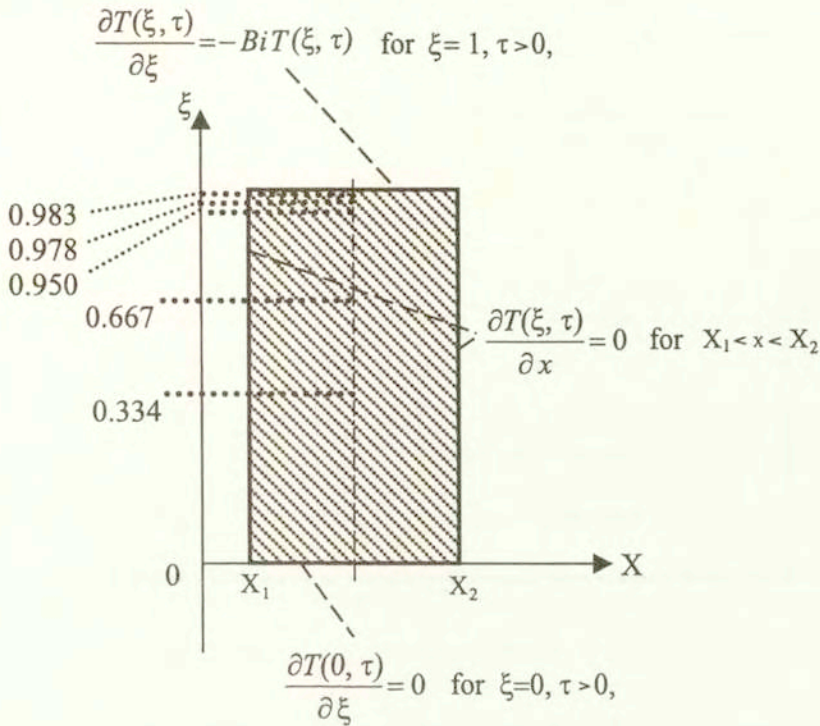


FIG. 3. The cross section of analysed solid with boundary conditions and measurement points locations.

4. Experimental apparatus

Schematic diagram of the test set-up with the most important working sections like: fan inducing air flow, open wind tunnel generating axisymmetrical jet, measurement sensors and record circuit, is shown in Fig. 3.

The diameter of the outlet nozzle of the wind tunnel was selected to emit impinging cooling jet where the diameter was larger than the one of the analysed specimen, in order to ensure smaller change of the temperature along the radius of the cylinder with respect to the axis temperature of the cylinder. The surface of the analysed specimen was placed in the axis of the cooling jet, at the distance of 2D (D-diameter of the nozzle) from the outlet nozzle section. The jet impinges the plate where the analysed solid was placed. During experimental studies, the diameter of the nozzle as well as the distance between the analysed solid and the outlet nozzle section were constant.

At the first stage of the experiment, a plate made of polystyrene isolated the heat exchange surface. After heating the specimen to the temperature of 100°C,

the plate was rapidly removed starting the cooling process with impinging air jet (the remaining heat exchange surfaces were insulated).

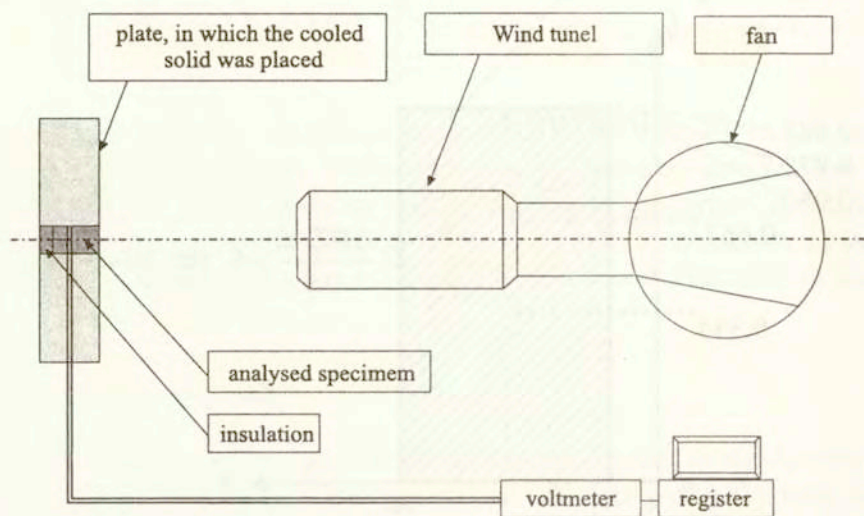


FIG. 4. Schematic diagram of the test rig.

During the experimental analyses, variation of the temperature inside the solid was monitored with Cu-constantan thermocouple. The measurements of the average velocity of the coolant flow were accomplished by the measuring nozzle and the pressure differences processor Furness Control FCO-14. The measurement data were recorded by applying voltmeter Keithley 2000 under the supervision of the LabView computer application.

5. Sensitivity of the solution of the inverse heat conduction problem to the random temperature measurement errors

During intensive heating/cooling processes the changes of the temperature inside the solid are smothered and delayed in time to the changes of the temperature on the heat exchange surface. As a consequence, small errors in temperature measured inside the solid are enlarged. They appear as large oscillations in determined values of the boundary conditions on the heat exchange surface.

For the purpose of showing the sensitivity of the solution of the inverse heat conduction problem to the random temperature measurement errors, the temperature field satisfying stationary equation in cylindrical co-ordinate system

$$(5.1) \quad \frac{\partial}{\partial \xi} \left(\xi \frac{\partial T}{\partial \xi} \right) = 0$$

was analysed. In this case, the temperature measurements were disturbed in 0.5%. The temperature field fulfilling stationary Eq. (5.1) has the solution

$$(5.2) \quad T = T_2 + \frac{T_1 - T_2}{\ln \frac{\xi_1}{\xi_2}} \ln \frac{\xi}{\xi_2} = T_2 + g \ln \frac{\xi}{\xi_2}.$$

The value of the temperature gradient containing the random temperature measurement errors was determined as

$$(5.3) \quad g_b = \frac{T_1 - (T_2 + \delta T_2)}{\ln \frac{\xi_1}{\xi_2}}.$$

The deviation between the temperature gradient containing the random temperature measurement errors and the exact temperature gradient was determined as

$$(5.4) \quad \delta_G = \sqrt{\frac{(g_b - g_{\text{exact}})^2}{g_{\text{exact}}^2}}.$$

The schematic distribution of the temperature determined by means of the undisturbed temperature measurement and the schematic distribution of the temperature determined by means of the disturbed temperature measurement are shown in Fig. 5.

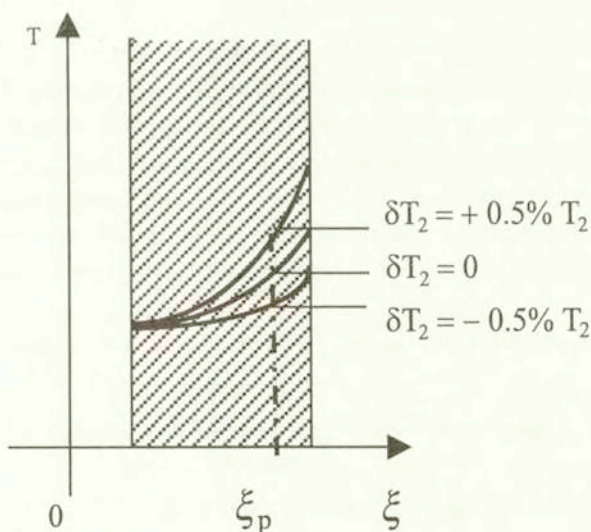


FIG. 5. Temperature distribution.

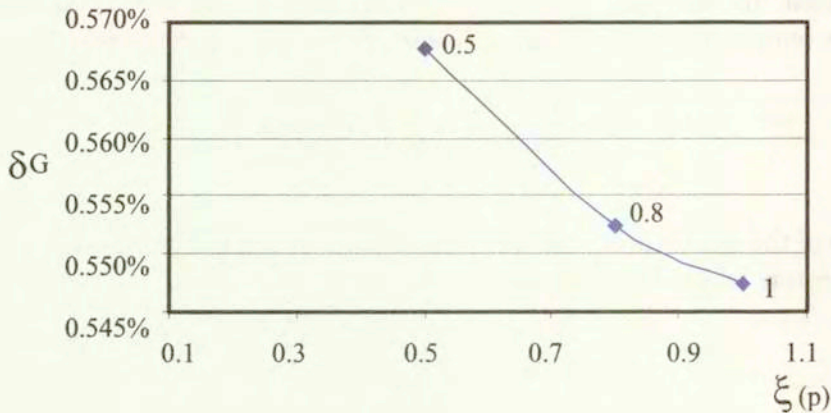


FIG. 6. The distribution of δ_G .

The increasing value of deviation of the temperature gradient as the increase of the distance of the measurement point location from the heat exchange surface is shown in Fig. 6.

The reconstruction of the boundary conditions on the basis of distorted measurements is a very complicated subject and susceptible to random temperature measurement errors [13].

6. Temperature distribution of the analysed solid

The results of the analysis of the inverse heat conduction problem were obtained by applying the temperature data measured at one point inside the solid, 1mm from the heat exchange surface. By introducing the temperature measurements to the computer application written in programming language – Fortran 77, solving the inverse heat conduction problem, the temperature distribution in the analysed solid was determined. The solution of the inverse problem was compared with temperature measurements taken inside the solid in five points Fig. 7.

Accuracy of the solution of the inverse problem was determine by means of

$$(6.1) \quad \delta_\theta = \sqrt{\frac{(T_{\text{measured}} - \theta_{\text{inverse solution}})^2}{T_{\text{measured}}^2}}$$

The standard deviation δ_θ varies from 0.10% to 1.25%.

The temperature measurements applied to solve the inverse heat conduction problem significantly influence the determination of the heat flux transferred from the analysed solid to the cooling air jet.

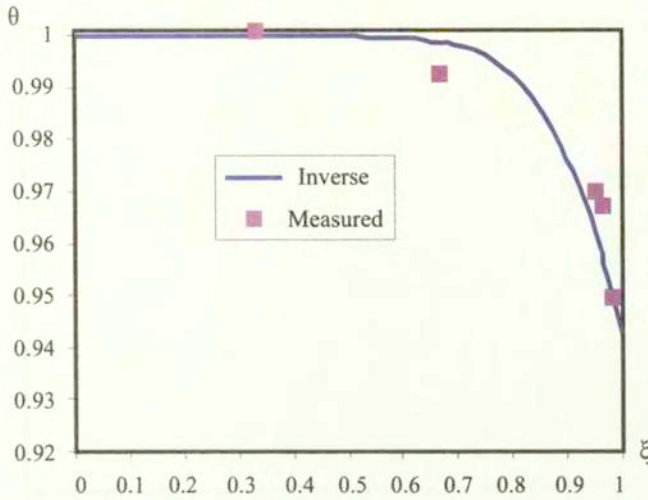


FIG. 7. Temperature distribution inside the analysed solid after 15s from the beginning of cooling.

7. The temporary Bi number values

On the basis of determined temperature distributions, applying the heat functions properties, the Bi number distributions during the cooling process were reconstructed

$$(7.1) \quad Bi = \frac{\frac{\partial \theta(1, \tau)}{\partial \xi} \Big|_{\xi=1}}{\theta(1, \tau)} = \frac{\sum_{i=1}^N \left(\sum_{n=1}^N U_{ni} v_{n-1}(1, \tau) \right) \theta(\tau) \Big|_{\xi=1}}{\theta(1, \tau)}$$

The temporary Bi number values, shown in Fig. 8, slowly rise until the heat flux conducted on the surface of analysed solid achieves the maximum value which can be taken over by cooling air jet.

The fluctuations in the Bi number distribution are caused by sensitivity of the solution of the inverse heat conduction problem to the random temperature measurement errors. For that reason, the elimination of the random temperature measurements errors by appropriate approximation of the measured temperature distribution is essential.

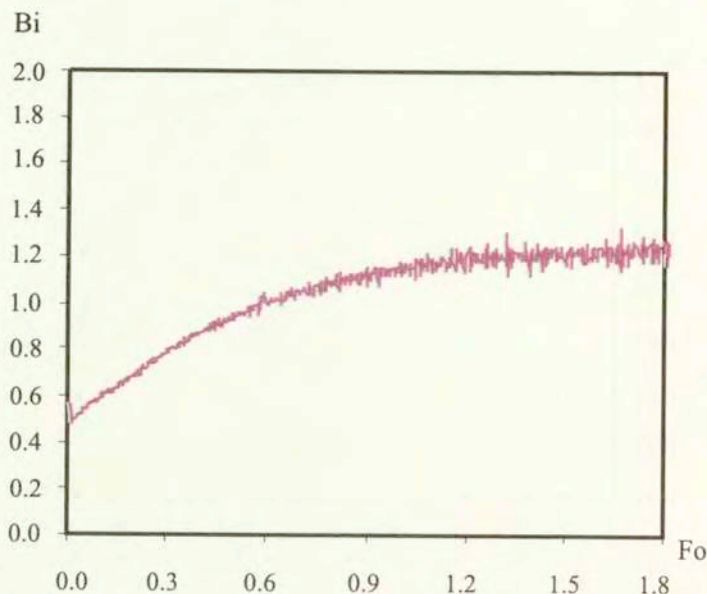


FIG. 8. The temporary Bi number values calculating on the basis of distorted temperature data.

8. Elimination of the random temperature measurement errors

For the purpose of obtaining the Bi number distribution devoid of fluctuation, the measured temperature distribution is approximated by the second-degree polynomials and by the $e^{\gamma\tau}$ function. The results of the Bi number distribution calculated on the basis of the approximate data were shown with the Bi number distribution calculated on the basis of the measured data, to demonstrate the effectiveness of the applied approximation.

The results of the Bi number distribution calculated on the basis of approximation of the temperature distribution by the second-degree polynomials, shown in Fig. 9, are not satisfying. The approximate Bi number values after achieving maximal value are decreasing, causing distortion in the Bi number distribution. In order to avoid unfavourable properties of the approximation of the second degree polynomials, the approximation of temperature distribution by the $e^{\gamma\tau}$ function was applied. On the basis of the results of Bi number distribution, shown in Fig. 10, it was confirmed that the approximation of the temperature distribution by the $e^{\gamma\tau}$ function gives a satisfactory solution.

Averaging of the temperature measurements taken inside the solid is another method of decreasing the influence of the random temperature measurement errors on Bi number distribution.

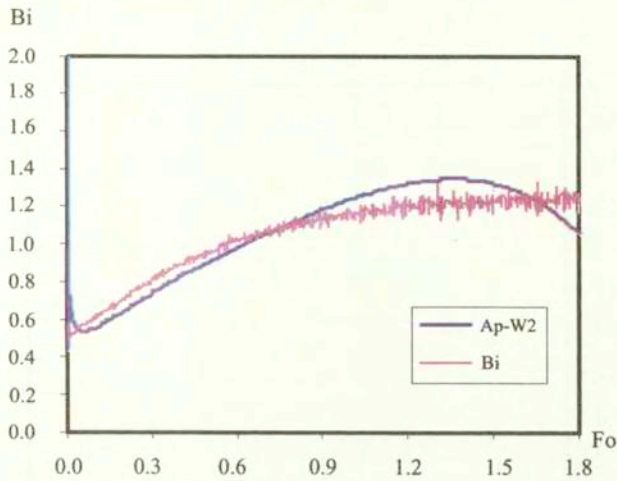


FIG. 9. The Bi number distribution approximated by second-degree polynomials.

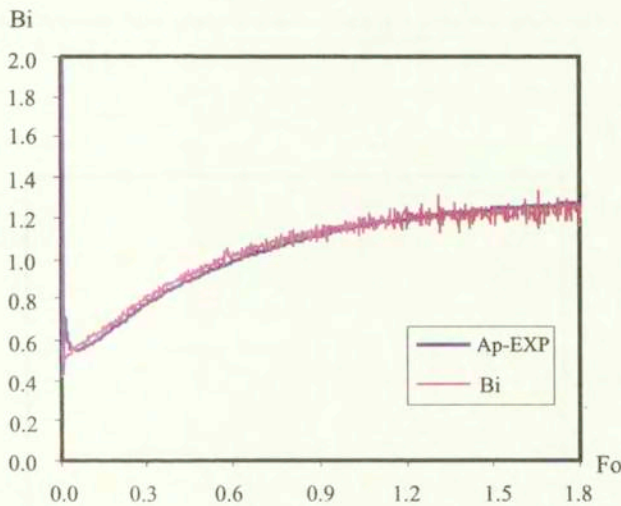


FIG. 10. The Bi number distribution approximated by $e^{7\tau}$ function.

The fluctuation in the Bi number distribution calculated from the averaged temperature measurements, demonstrated in Fig. 12, is significantly smaller than the fluctuation in the solution calculated from the single temperature measurement, shown in Fig. 11. The application of averaged temperature measurements taken inside the solid to calculate the Bi number distribution reduces the influence of the random temperature measurement errors on the Bi number distribution.

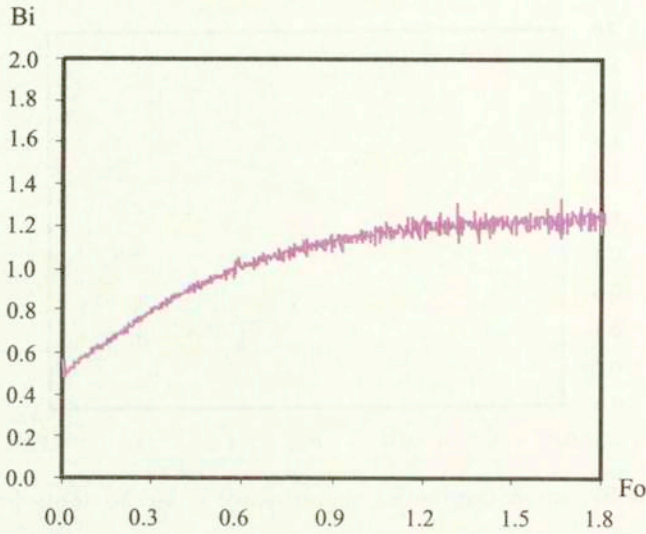


FIG. 11. The Bi number distribution calculated on the single temperature measurement.

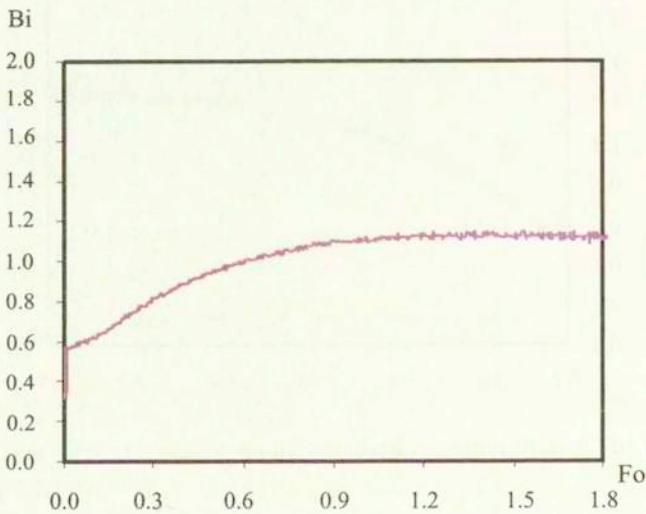


FIG. 12. The Bi number distribution calculated on the averaged temperature measurements.

9. The distribution of the heat transfer coefficient

The definition of the Bi number was applied to determine the heat transfer coefficient

$$(9.1) \quad h = \frac{Bi_{av} k_s}{Z}$$

The comparison of the heat transfer coefficient h determined from the solution of the inverse problem (the temporary Bi-number values) with the data given in the literature is shown in Fig. 13. The heat transfer coefficient h from the solution of the inverse problem was determined by averaging the Bi number, after the maximum value is reached by the heat flux which is taken over by the cooling air jet.

Literature data were applied to determine the accuracy of the presented method. The discrepancies in the distribution of heat transfer coefficients known from the literature are shown in Fig. 13. The author of the paper [1] claims in his works that the discrepancies in heat transfer coefficients distributions in the literature are caused by the errors which appeared during experiments, and by the variability of the structure of the jets generated by the differently shaped emitters and nozzles, the details of which are not mentioned in the publications. In consequence, there are discrepancies in heat transfer coefficients distributions in the literature data shown in Fig. 13

The values of heat transfer coefficients following from the solution of the inverse problem were compared with the data published in paper [1]. These data [1] were determined on the basis of the experimental research led in the Chair of Thermal Engineering, accomplished by applying the same test set-up which was used to obtain the data to solve the inverse problem. The air impinging jet was generated by applying the same nozzle. The accuracy of determination of the heat transfer coefficient h from the solution of the inverse heat conduction problem compared to the data from paper [1] was determined by

$$(9.2) \quad \delta_h = \sqrt{\frac{(h_{[1]} - h_{\text{inverse solution}})^2}{h_{[1]}^2}}$$

The standard deviation δ_h varies from 0.37% to 4.07%.

Comparison of the heat transfer coefficient h , determined by the solution of the inverse problem – calculated by applying average of nine temperature measurements taken inside the solid, with the date known from literature, is shown in Fig. 14.

The standard deviation of the solution of the inverse heat conduction problem – calculated by applying average temperature measurements with relation to data given in paper [1] was determine by

$$(9.3) \quad \delta_h = \sqrt{\frac{(h_{[1]} - h_{\text{inverse solution}})^2}{h_{[1]}^2}} = 2.08\%$$

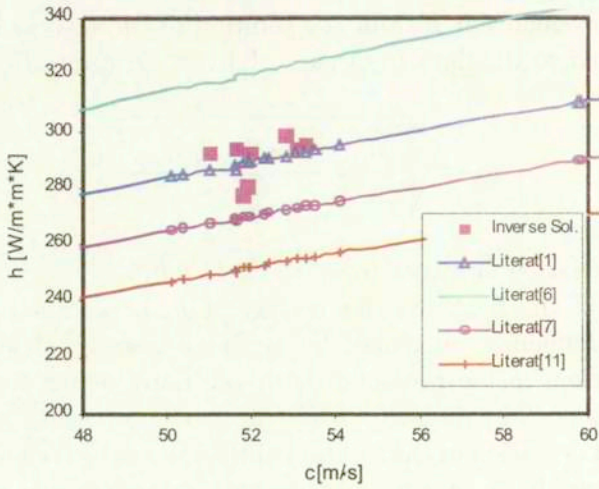
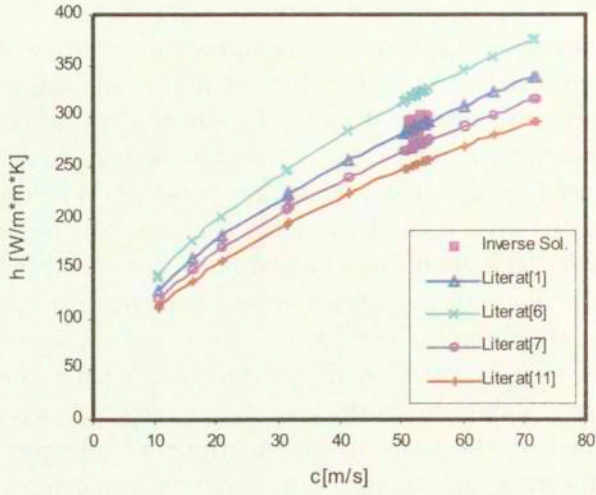


FIG. 13. Values of the heat transfer coefficient.

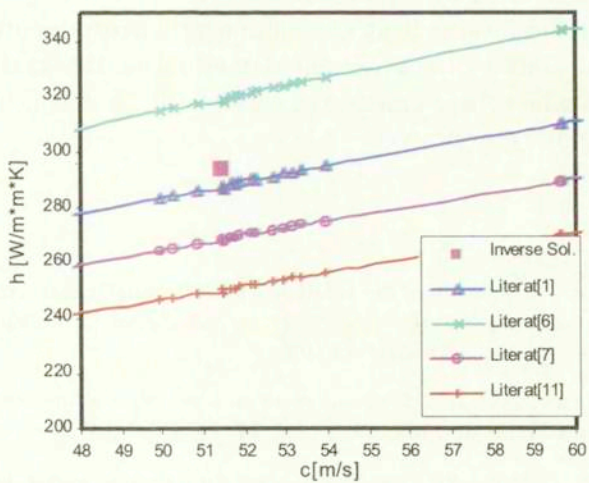
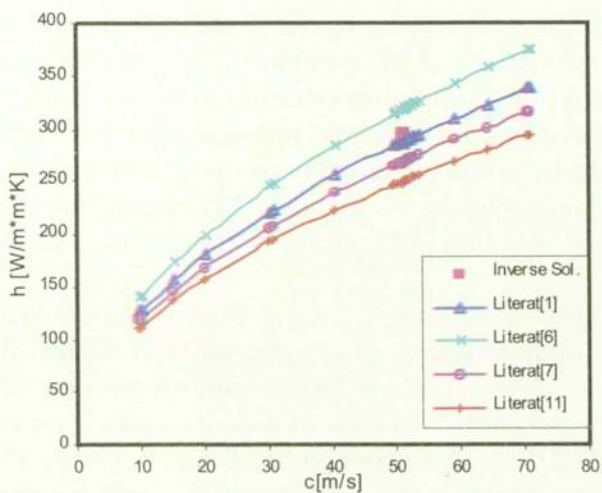


FIG. 14. Values of the heat transfer coefficient for the averaged data.

10. Conclusions

The investigation was aimed at determination of the properties of the solution of the inverse heat conduction problem occurring in real conditions. The inverse heat conduction problem is solved by using the heat functions applied to formulate the base functions of the Finite Element Method.

Because of the sensitivity of the solution of the inverse heat conduction problem to the random temperature measurement errors occurring during laboratory and industrial experimental studies, the approximation properties of the temperature measurement by using the second degree polynomials and the $e^{\gamma\tau}$ function were demonstrated. It is necessary to stress that by applying the approximation of the temperature distribution by means of the $e^{\gamma\tau}$ function, we obtain satisfactory results.

Application of the averaged temperature measurements taken inside the solid in order to calculate inverse heat conduction problem reduces the sensitivity of the solution of the inverse problem to the random temperature measurement errors.

The properties of the heat functions were used to reconstruct the heat transfer coefficient on the heat exchange surface. On the basis of a comparison with the data known from the literature, the accuracy of the reconstruction of the heat transfer coefficient is considered as satisfactory.

The results of the inverse heat conduction problem presented in this paper confirm the applicability of the presented method to the analysis of the heat exchange process when direct measurements of the heat transfer coefficient or the heat flux cannot be performed.

References

1. L. BOGUSŁAWSKI, *Estimation of the possibility of heat transfer measurement at stagnation point with constant temperature anemometer surface sensor* [in Polish], VIII Symposium of Heat and Mass Transfer, Białowieża 1992.
2. S. CHANTASIRIWAN, *Inverse determination of steady-state heat transfer coefficient*, International Journal of Heat and Mass Transfer, **27**, 8, 1155-1164, 2000.
3. CHING-YU YANG, *Solving the two-dimensional inverse heat source problem through the linear least-squares error method*, International Journal of Heat and Mass Transfer, **41**, 2, 393-398, 1998.
4. M. CIAŁKOWSKI, *Solution of a non-stationary inverse problem of heat conduction by means of new type base functions of finite element method* [in Polish], XVII Symposium of Thermodynamics Kraków 1999.
5. M. CIAŁKOWSKI, A. FRĄCKOWIAK, *Heat functions and their application to the solution of heat conduction and mechanical problems* [in Polish], WPP, Poznań 2000.

6. R. GARDON and J. COBONQUE, *Heat transfer between a flat plate and jets of air impinging on it*, Int. Heat and Mass Transfer Conference, Univ. Colorado, p. 454, 1961.
7. W. M. KAYS, *Convective heat and mass transfer*, Mac Graw Hill, 1966.
8. D. LESNIC, L. ELLIOTT, B. INGHAM, *The solution to an inverse heat conduction problem subject to the specification of energies*, International Journal of Heat and Mass Transfer, **41**, 1, 25-32, 1998.
9. LIU LINHUA, TAN HEPING and YU QIZHENG, *Inverse radiation of temperature fields in three-dimensional rectangular furnace*, International Journal of Heat and Mass Transfer, **26**, 2, 239-248, 1999.
10. NEHAD AL.-KHALIDY, *On the solution of parabolic and hyperbolic inverse heat conduction problems*, International Journal of Heat and Mass Transfer, **41**, 3731-3740, 1998.
11. C. POPIEL and L. BOGUSŁAWSKI, *Effect of flow on the heat or mass transfer on a plate in impinging round jet*, Sc. UK Nat., Conference on Heat Transfer, p. 663, Glasgow 1988.
12. B. SAWAF, M. N. ÖZISIK, *Determining the constant thermal conductivities of orthotropic materials by inverse analysis*, International Journal of Heat and Mass Transfer, **22**, 2, 201-211, 1995.
13. J. TALER, P. DUDA, *Experimental verification of space marching methods for solving inverse problems*, Heat and Mass Transfer, **36**, 324-331, 2000.
14. M. WOELKE, A. FRĄCKOWIAK, *Stability analysis of the solutions of the heat conduction inverse problem* [in Polish], XI Symposium of Heat and Mass Transfer, Gliwice - Szczyrk 2001.

Received April 24, 2002;
